Skoltech

Skolkovo Institute of Science and Technology

MASTER'S THESIS

Optimization of coating process in deformable roll coating systems by means of fluid flow simulation of non-Newtonian liquids

Master's Educational Program: Information Science and Information Technologies (Advanced Manufacturing Technologies)

Student_____

Anastsija Cumika

Research Advisor:_____

Ighor Uzhinsky

Full Professor

Co-Advisor:_____

Michail Gusev

Researh Scientist

Moscow 2021

Skoltech

Skolkovo Institute of Science and Technology

МАГИСТЕРСКАЯ ДИССЕРТАЦИЯ

Оптимизация процесса окраски в системе с деформируемыми валками с использованием методов моделирования потоков не-ньютоновских жидкостей

Магистерская образовательная программа: Информационные Системы и Информационные Технологиии (Передовые Производственные Технологии)

Студент_____

Анастасия Чумик

Научный руководитель:_____

Игорь Ужинский

Старший Пеподователь

Со-руководитель:_____

Михаил Гусев

Научный сотрудник

Москва 2021

Optimization of coating process in deformable roll coating systems by means of fluid flow simulation of non-Newtonian liquids

Anastsija Cumika

Submitted to the Skolkovo Institute of Science and Technology
on June 9, 2021

Abstract

The roll to roll deformable coating systems with non-Newtonian fluids have been studied for many years since the last century, however there are few good numerical models performed on this topic, especially the ones that could be used in the industrial applications. Most of the researchers have focused on the methods and result analysis, rather than scalability and industrial application. For the industry the study of the coating thickness is important because paint is a consumable, and all the wasted paint during the production are wasted money. Therefore, this work focuses on the research of the methods for the numerical model of the roll to roll coating system with the coating thickness as a target output parameter.

In this study, the 18.2 Ansys software was used for the simulation. Ansys Structural was used to for the elasomter model development, based on the experimental results of the deformable coater layer. Ansys Fluent was used for the fluid domain of the system, where the VOF (Volume of Fluid) multiphase model was implemented to simulate the free surface of the paint. Methods to solve the numerical solution were chosen to maximize the precision of the air and paint interface for a better precision of the model.

As a results, the domain, geometry, mesh and boundary conditions of mechanical, fluid and coupled system were developed. The model with the best coefficients for the non-Newtonian paint and applicator roll elastomer was chosen and implemented in the solution. The results were obtained for both regular and non-Newtnian fluids as a function of support roll speed, applicator roll speed and separation distance between the rolls. Through the research, also the architecture for the recommendation system was proposed. All the performed work lies as a grounding foundation for the roll to roll coating recommendation system.

Research Advisor:
Name: Ighor Uzhinsky
Degree: P.h.D.
Title: Full Professor

Co-Advisor:
Name: Michail Gusev
Degree: P.h.D.
Title: Researh Scientist

Acknowledgments

I want to acknowledge all the people that supported me through this research and enabled me to write this thesis.

First I want to thank the Skoltech CDMM research center, especially my research adviser Prof. Ighor Uzhinsky, who suported me with advice on my work and research, and Michail Gusev, who proposed this topic to me, guided me throughout the whole research, and helped me to find the right people for the support. Also, I want to stated out Daniil Padalitsa, who helped me with learning Ansys software and supported me with the advises on my model development. Besides that, I want to thank Alexander Digilov, who worked on the elastomer model optimization, which was important for this research and further development. Special thanks, to the NLMK roll coating expert for the data provided of the deformable roll to roll coating system, non-Newtonain paint fluid parameters and experimental data of the applicator roll elastomer.

Finally, I want to thank my dad who always supports me in all my beginnings and truly believes in me.

Contents

List of Figures

List of Tables

Chapter 1

Introduction

1.1 Background

In the industry there are multiple techniques used to apply a coating on a surface, such as roller based transfer coating, slide coating, slot coating and die coating [3]. Roll coating techniques have been used in the wide variety of fields for over a 100 years to apply a thin layers of the substrate to the continuous web/sheet such as paper, films, plastic, textile or metal. The process involves the moving of the web between the two rotating rolls. More rolls might be used for the metering or substrate pick up purposes. The application of the roll coating include photographic films, medical x-rays, audio and video magnetic tapes, electronic printed circuits, flexible solar panels and displays, membranes, adhesive tapes, as well as decorative or protective coatings. Roll coating is also used in chemistry and biology industries.

1.1.1 Roll coating in steel making

In the steel making industry roll to roll coating is used at the cold rolling plant, where the steel sheets are coated with multiple layers of coating, that helps to prevent corrosion, hide joints and seams, as well as for surface physical protection and pretty colors. The typical three layer coating consists of pretreatment, which prepares the surface for the further coatings,prime coating, that inhibits corrosion and created a good adhesion properties, and top coat, that provides 1_{st} defence protective properties from the environment and the facade of the sheet [1]. Based on the application, different coatings are used, where as well an intermediate layer might be used, to create extra thickness for the extra protection. The Coated steel metals sheets are used for the variety of applications starting from household appliances and up to sport cars.

On the roll coating line, which is shown in figure 1.1, the sheet undergoes a full cycle that starts with uncoiling and ends with recoiling. Besides the coating, the sheet is also cleaned, cured in the oven and dried out. At the end of the line we get a ready to sell coated steel sheet coil.

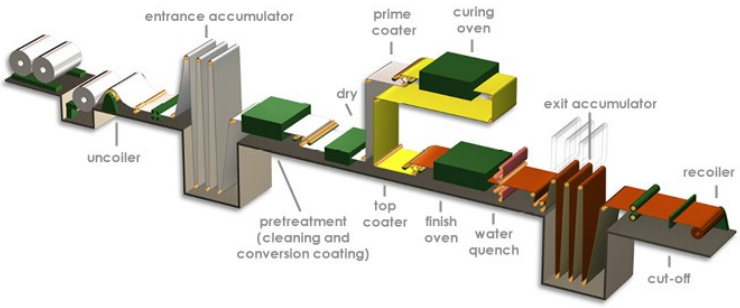

Figure 1.1: The schematic of the full roll to roll coating system (adapted from [1])

1.2 Research motivation

NLMK (Novolipetsk steel company) is a global steel company. In their Lipetsk plant in the cold rolling shop the steel sheet deformable roll to roll coating is performed. Most of their coated sheets are used for the household appliances. Even though, the application is common, the paint used for the coating is an expensive, non-Newtonian fluid coating ordered from Europe as a special order. There is usually the minimum thickness that is set by the customer, so that they won't accept the sheets whose coating thickness is less than minimum required. Therefore, the company faced a problem that often due to imprecise calibration the overspending of coating occurs. The thicknesses of the coating are usually 20-25 μm. Overshooting by 4-5 μm leads to the loses of approximately 50 mil. Rubles per year for the company. NLMK wanted Skoltech to find a solution that would help set a more precise calibration and optimize the roll to roll coating system on their plant.

1.3 Research gaps

Facing the motivation stated above, the research was performed. Even though the roll to roll coating topic if popular among the researchers, most of the research was done in the 20^{th} century or early 00's. Most of the works were oriented on the research of the methods and approaches to solve the complicated problem. The main goal was to find a way and to develop and approach. As we are interested in the solution for the industrial, application and we have found few research paps from our point of view:

- **Focus** - there was almost no research that would focus specifically on the analysis of the thickness parameter, studying how it changes in various systems and setups. On this topic we could point out only B.Willinger, A.Delgado, and B.Grashof works [4, 5] and
- **Scalability** - the research performed by the most scientists is done to reach a specific goal, however, often their approaches are computationally ineffective or are hard to implement for the everyday usage of the problem, such as industrial application. The only industry oriented

study in the steel making field was done by FMP Technology Company together with AG Demmel Company published in summer 2020 [6].

- **Optimization -** since there was no focused research targeted on the film thickness, especially containing scaleable approaches, no one performed the optimization of the roll to roll coating process.

1.4 Research aim, objectives and questions

This research is focused on the deformable roll to roll coating thickness investigation based on the input operational parameters. The main aim of the research is to Build the foundation of the roll coating process recommendation system that would be used in the industrial applications to optimize the processes on the plant

Thesis objectives include:

- Development of the numerical coupled model of the deformable coating process
- Obtaining data for the thickness measurements for different parameters of the model such as roll speeds and distance between the rolls/force of the applicator roll
- Maintain the scalability factor for the methods used in the research

As a part of out research we want to answer the questions that would help us to reach the main goal not only this work, but also the global goal of the project. We start with researching what roll coating is and how the numerical formulation was done before? We also want to know what methods and models should we choose to solve out problem? What parameters affect the paint thickness and how? Keeping in mind the industrial application, we have to find an answer on how to set up a model to get scalable results. Finally, since there are only 2 parameters that we can really control on the coating system, we want to specifically know, how roll speeds and distance between them/applicator force affect the coating thickness?

In order to reach the goal the following steps were performed:

1. Researched the literature on the deformable roll to roll coating to got the understanding of the system. Studied the approaches used to solve the problem, especially in the last ten years.
2. Preformed the data analysis provided by the NLMK company
3. Got acquainted with the FE analysis as a topic and performed basic tutorials to understand basic concepts. Created a simple deformation model for the applicator roll elastomer.

4. Got acquainted with the CFD modeling and studied the ANSYS Fluent interface. Learned to build complex mesh settings.
5. Studied the theory of the multiphase modeling topic (Volume of Fluid models) and non-Newtonian liquid models (Power law)
6. Built the geometry of the domain and perform meshing/
7. Implemented of the 2D CFD model of the forward roll coating with rigid roll and regular paint, using the multiphase modeling in ANSYS Fluent.
8. Found the coefficient parameters for the non-Newtonian fluid material model using the provided measurement of the selected paints.
9. Implemented of the 2D CFD model of the forward roll coating with rigid roll and non-Newtonian paint, using the multiphase modeling in ANSYS Fluent.
10. Performed the optimization FE study, to select the best model and its parameters for the elastomer.
11. Study and implement the solution for the automatic paint thickness measurement on the rolls
12. Create a 3D domain geometry and mesh, where both mechanical and fluid domain share the same interface/
13. Study and implement the coupled model solutions. Generate and analyze the results

The general goal of the project is to create a recommendation system for the that roll to roll coating that would be integrated in the industrial application ,and bring the positive business effect to the company by saving the money via the precise parameter preset for the coating system.

1.5 Thesis structure

This thesis includes the Introduction, main part (literature review, our system analysis, methodology, results and discussion), and conclusion with suggestions for further work.

Chapter 1, the introduction to the thesis, describes the background of the roll to roll coating in the steel making industry, research motivations, gaps, aim, objectives and questions, with the detailed plan of the work.

Chapter 2 is an extensive literature review on this topic where the types of roll to roll system along with the conducted research on this topic, both experimental and numerical are described.

Chapter 3, our system analysis, describes in detail the general coating system, along with the coating system unit. There we also analyze, the provided by NLMK data, to get the understanding of the expected parameters of the processes.

Chapter 4, is the step by step explanation of the methodology of the thesis. There are 3 parts: mechanical part, fluid part and system coupling. For each part geometry, mesh and setup development is described.

Chapter 5, is the result section of the research, where we discuss the achieved results on the independent models as well as grand result of the coupled model. Also, there is a discussion sections and suggestions upon the further steps that must be accomplished to finish the product as recommendation systems.

Finally, the last part of the research is devoted to the conclusion and suggestions for further work.

Chapter 2

Literature review

2.1 Types of the roll coatings

There are multiple types of the roll coating existing. Depending upon the direction of rolls rotation, roll coating is classified as forward roll coating and reverse roll coating. In the forward roll coating the surfaces move in the same directions, which means that application and support rolls are rotating in the opposite directions (counter rotating rolls), as shown in figure 2.1 on the left schematics. On the forward roll coating there has been a lot of theoretical studies in the 90s that have a good agreement with experimental results[7].

In the reverse roll coating the surfaces move in the opposite directions, so application and support rolls rotate in the same direction (co-rotating rolls), as shown in figure 2.1 on the right. Reverse roll coating can produce thinner and more stable coatings than forward roll coating. However, in the use of deformable roll coating, it increases the wear of the elastomer.

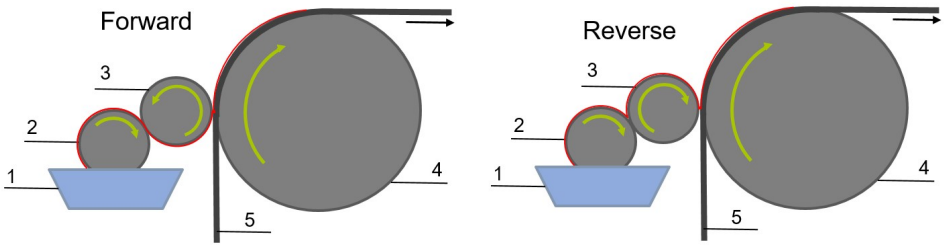

Figure 2.1: Forward roll coating (left) and reverse roll coating (right) scheme. 1. Paint with paint; 2. Steel pick-up roll; 3. Rubber applicator roll; 4. Steel support roll; 5. Steel sheet

Roll coating can be performed with rigid rolls and positive gap, as well as with deformable rolls with negative or positive gap. To achieve the negative gap, a steel roll with an elastomer cover ,pressed against the steel support roll, is used, therefore, the distance between the centers of the rolls, is smaller than the sum of the rolls radii. The representation of positive [8] and negative gap [5, 9, 10, 11] settings is shown in figure 2.2. Operating with deformable rolls with negative gap is widely used in the industrial applications, because it provides more stable and thinner coatings [2]. When working with deformable gap studies, one has to consider the theory of structural deformation of the elastomer. Such studies were done many years in 50s and 60s [12, 13], and is a basic theory

of structural dynamics. There exist multiple models that can be used to describe the behavior of the elastomer and these will be discussed later in this work.

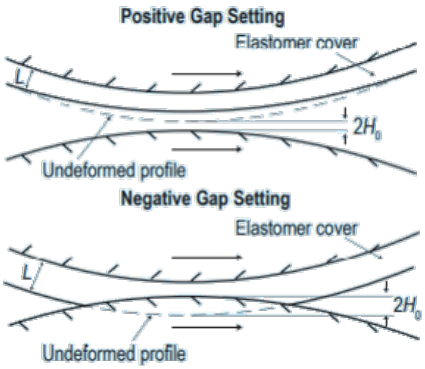

Figure 2.2: Positive and negative gap nip representation [2]

Roll coating also can operate in flooded [14, 15]and starving regime [15]. When operating in the flooded regime, the incoming film volume exceeds the minimum clearance [15]. In addition, the roll coating can be operated using pan-fed, fountain roll-fed, nip-fed, and slot die-fed methods[16]. Some applications might include a metering roll that takes off the extra coating and allows extra control for the coating thickness and stability. The summary of the different typed of the roll coating systems is shown in table 2.1.

Table 2.1: the segmentation of the roll coating systems

Way of differentiation	**Types of roll coating**
Roll rotation	Forward or reverse
Applicator roll surface	Rigid or deformable
Rolls separation distance	Positive or negative gap
Volume of coating at the nip	Flooded or starving regime
Coating feeding	Nip or Pan fed

2.2 History of the research

Most of the roll to roll coatings studies were done in the previous century. There are few researchers that have published many papers on this topic. In the period from 1987 till 1997, Coyle has studied the theory of both forward [17, 18, 19, 20] and reverse [21, 22, 23] roll coating , and some of his publications are oriented towards the non-Newtonian liquid coatings [22, 21, 18, 20]. Important to note, that Coyle also focused on film splitting region in his early works [17, 18, 19] and even in 1982 performed a computer simulation of the nip flow [16]. The film splitting region is very complicated but important part of the model, because it directly affects the accuracy of the coating thickness result. In the most recent research, Coyle has also focused on the stability of the coating [19, 7].

Carvalho and Scriven had their first article on roll coatings in 1994 and all of his research was oriented towards the deformable forward roll coatings, including his Phd thesis. Studies included topics like how deformable roll [24, 25, 26] and its properties [27] affects the flow and coating stability, and what models to be used to represent the elastomer [28]. Coyle, Carvalho and Scriven laid down the basics of the numerical and analytical research for the roll to roll coating, and most of the later research was based on their work.

Another person, who performed a lot of research on roll coatings was Benkreira. In his early work, performed in the period of 1981 to 1994, with Edwards, M.F., Benkreira devoted his work towards the development of the model for the forward roll coating [29], and performed the experiments for purely viscous fluids [30] and non-Newtonian fluids [31]. Recently Benkreira and Shibata, Y. published two more studies, in 2013 on the high speed reverse roll coating [32] and in 2017 a great study on the deformable reverse roll coating, where he clearly showed mathematical formulations and compared his calculations with his own experiment [10].

As one can see, the topic of roll to roll coating is rather popular and scientists still do research on it. The goal of the research most often is to find a model that would precisely predict the output parameters such as pressure distribution and coating thickness. For the applications, it is important to know what operational parameters affect target parameters the most. In his review, Abbot stated that main influencing parameters are viscosity, roll velocity, elasticity of deformable layer, and load or initial overlapping distance [2]. Grashof did a specific study based on the analytical calculations where he was discovering what parameters have the most influence in the deformable roll coating. He proved Abbot, findings, and also stated that rubber thickness might also have the influence, for Newtonian fluids [5].

2.3 Numerical research in roll to roll coating

Regarding the numerical studies, many authors have applied lubrication theory simplifications to solve the Navier-Stokes equations. One of the first authors to publish a work on solving such a problem were Greener and Middleman in 1975 [33]. Carvalho and Scriven [24, 27] and Coyle [20, 18, 23] have also used the lubrication approximation in their work. Even in late works lureication approximation is still used, for example, Ali N. used it in his analytical research that was performed in mathematica software [34]. Lubrication approximation has showed to be a reliable method, so even in recent works authors have used this approach [35, 36, 37]. In some of the articles, Carvalho and Scriven worked on solving a full two dimensional Navier-Stokes equation by the Galerkin / finite element method [26, 28].

While lubrication approximation gives a good result, a numerical simulation, that solve a full Navier-Stokes equations, can give more insights about the flow in the roll to roll coating.

Numerical simulation for such a system might be computationally expensive, therefore up to day there is not many works published that involve numerical simulation. One of the first scientists to perform the numerical simulation was Coyle in 1982 utilizing Galerkin finite element method which induced 39 elements with 440 equations [16]. Resulting set of non-linear algebraic equations was solved using Newton's method. Coyle continued to utilize and improve this technique in his further works. In 1999 Hao extended the Coyle research to get more insights about the parameters influence and flow behavior in the reverse roll coatings [38]. In 2000's Chandio and Echendu have used semi-implicit Taylor-Galerkin/Pressure-correction algorithm to solve momentum and continuity governing equations [39, 40]. Echendu had 1550 elements in his medium mesh; comparing to Coyle's 39 elements in 1982, that is a great precision improvement.

2.3.1 Multiphase models

This type of problem can be solved as a multiphase system. We have two phases: air and paint, and we are inspecting the free surface development at the meniscus. There are multiple model for multiphase system, but when working with multiphase the VOF (Volume of Fluid) is the best option. Few authors have specified that they used this model and both od them mentioned using SIMPLEC algorithm to solve the system of finate-volume equations [41, 42]. The only work that was found to be solved in Ansys with VOF model was Jang and Chen research perfromed in 2009 [41]. Ansys has published a documed that describes the best practices in modeling a thin liquid coatings. There Ansys developers mentioned the only VOF model is recommended for solving such problems in Ansys [43]. The manual for the theory of Ansys fluent answers the question of why we should choose VOF: "...a surface-tracking technique applied to a fixed Eulerian mesh. It is designed for two or more immiscible fluids where the position of the interface between the fluids is of interest" [44].

In VOF model the fluids (phases) are not interpenetrating. In each cell the volume fraction of the cell is computed and the q^{th} fluid's volume fraction (secondary phases) it is denoted as α_q. The following conditions are possible [44]:

- $\alpha_q = 0$: the cell is empty of the q^{th} fluid
- $\alpha_q = 1$: the cell is full of the q^{th} fluid
- $0 < \alpha_q < 1$: the cell contains interface between the q^{th} and one or more fluids.

The tracking of interface is accomplished by the solution of the continuity equation for one or more phases [44]:

$$\frac{1}{\rho_q}\left[\frac{\partial}{\partial t}\left(\alpha_q \rho_q\right) + \nabla \cdot \left(\alpha_q \rho_q \vec{v}_q\right) = S_{\alpha_q} + \sum_{p=1}^{n}\left(\dot{m}_{pq} - \dot{m}_{qp}\right)\right] \tag{2.1}$$

where $\dot{m}$ is the mass transfer between the phases and S_{α_q} is a source term that is our case is 0. In two phase system, this equation is solved only for one phase - q, which is considered as a secondary phase. To calculate the primary phase volume fraction we use a simple constraint:

$$\sum_{q=1}^{n} \alpha_q = 1 \tag{2.2}$$

Since the paint thickness is vary small, we are interested in the sharp interface between the phases. Also, it would increase the precision of our work, as the paint thickness is our target parameter. VOF continuous equation can be solved with the implicit or Explicit scheme, and different methods are used for different schemes. In general, based on the research and the Ansys fluent user's guide, Method that gives you the clearest and cleanest interface is the explicit with Geometric-reconstruct [45]. The Geometric-reconstruction approach uses a piecewise-linear approach to represent the interface between the fluids. "It assumes that the interface between two fluids has a linear slope within each cell, and uses this linear shape for calculation of the advection of fluid through the cell face" [44] In addition, we are depended on time in our solution, as we want to see how paint propagates in time as the rolls rotate from the static position, the choice fell towards the explicit scheme with the following equation:

$$\frac{\alpha_q^{n+1}\rho_q^{n+1} - \alpha_q^n \rho_q^n}{\Delta t} V + \sum_f \left(\rho_q U_f^n \alpha_{q,f}^n\right) = \left[\sum_{p=1}^{n} \left(\dot{m}_{pq} - \dot{m}_{qp}\right) + S_{\alpha_q}\right] V \tag{2.3}$$

where n is the index of the previous step, V - volume of the cell, and U_f the volume flux through the face, based on normal velocity.

The material properties are tracked as an weighted average based on the volume fraction in each cell. For example the equation for density for each cell is shown in eq. 2.4, where 1 and 2 are the subscripts that represent the phases [44].

$$\rho = \alpha_2 \rho_2 + (1 - \alpha_2)\, \rho_1 \tag{2.4}$$

The momentum equation is solved for the whole domain, where the averaged material properties (as shown above) are used. The equation is a classical Navier-Stokes momentum equation[44]:

$$\frac{\partial}{\partial t}(\rho \vec{v}) + \nabla \cdot (\rho \vec{v}\vec{v}) = -\nabla p + \nabla \cdot \left[\mu \left(\nabla \vec{v} + \nabla \vec{v}^T\right)\right] + \rho \vec{g} + \vec{F} \tag{2.5}$$

The energy equation is also shared among the phases[44]:

$$\frac{\partial}{\partial t}(\rho E) + \nabla \cdot (\vec{v}(\rho E + p)) = \nabla \cdot (k_{eff} \nabla T) + S_h \tag{2.6}$$

2.3.2 Non-Newtonian liquid roll to roll coating

The fluid used in this research is a shear-thinning non-Newtonian liquid, which means that as the shear stress on the fluent increases, the viscosity of the fluid decreases. There are multiple models that could be used to represent a non-Newtonian material. In Ansys the following models are provided: power law, Carreau model, Cross model or Herschel-Bulkley model for Bingham plastics[45]. Jang and Chen have used the power law in their computations [41], while Kim have used the Carreau model [42]. All models can have temperature dependency that is described by the following equation:

$$H(T) = \exp\left[\alpha\left(\frac{1}{T - T_0} - \frac{1}{T_\alpha - T_0}\right)\right] \tag{2.7}$$

For our material the simple power law model was chosen that is described by the following equation:

$$\eta = k\dot{\gamma}^{n-1}H(T) \tag{2.8}$$

where k and n are parameters that are specific for each material. One can find these coefficients by performing the power fit on the experimental measurements of their material. k is the measure of the average viscosity of the fluid - consistency index, n is the measure of diviation of the fluid from Newtonian- the power law index. By looking at the power law index one can say what class does the fluid has:

- $n = 1$ - Newtonian fluid
- $n > 1$ - shear-thickening (dilatant fluids)
- $n < 1$ - shear-thinning (pseudo-plastics)

Based on the segmentation above, we expect our power law index to be less than zero.

2.3.3 Deformable roll – models for the elastomer modeling

As mentioned before, Carvalho and Scriven in the previous century were already modeling the deformable roll to roll coatings, where they also introduced the deformable models into their calculations. However, they introduced the deformation approximations into their equations, that did not directly take into account the specific material properties of the elastomer [20]. In later works the Young's modulus of the material is used in the dimensionless number such as elasticity number 2.10 which is used to measure the influence of hydrodynamic pressure to elastic restoring forces, and load number 2.9, which represents the ration of the applied load to the elastic restoring forces.

$$F = \frac{W}{ER_{eff}} \tag{2.9}$$

$$E_s = \frac{\mu U_{ave}}{ER_{eff}} \tag{2.10}$$

The R_{eff} is the effective radius of the system, that is computed from the applicator and support roll radii via the following equation:

$$\frac{1}{R_{\text{eff}}} = \frac{1}{2}\left(\frac{1}{R_1} + \frac{1}{R_2}\right) \tag{2.11}$$

These dimensionless numbers are used in the analytical computations [2, 5]. Lecuyer used the direct stress-strain tensor analysis with the elasticity matrix [14]. In this work the Mooney-Rivlin 2.12 and Blatz-Ko 2.13 hyperelastic models were studied and simulated via finite element analysis. The equations of these models are shown below:

$$W = C_{10}\left(I_1' - 3\right) + C_{01}\left(I_2' - 3\right) + \frac{1}{d}(J-1)^2 \tag{2.12}$$

$$W = \frac{\mu}{2}\left(I_2' + 2\sqrt{J} - 5\right) \tag{2.13}$$

ıhere W is the specific potential of elastic deformation of the material, I1 and I2 are first and second invariants of the tensor of the deformation measure, J - relative volumetric deformation, C10 and C01 are expansion coefficients of the elastic potential function in Maclaurin, μ - material shear modulus and d - material volumetric compressibility parameter. The specific potential W is used in the stress-strain tensor equation. In the general model, the pressure is passed to the mechanical model, that denoted the stress tensor, the strain tensor is computed which denotes the deformation and sets the interface shape between the fluid and solid boundaries.

2.4 Roll coating instabilities

It was mentioned, that based on the parameters, the coating might have the variety of instabilities. Figure 2.3 [19] shows the photo of the ribbing instabilities of the flow for the forward roll coating. In 1980 Greener performed the experimental study of ribbing instabilities for a rigid forward roll coating for a wide range of parameters to collect the data about the system [46]. Worth to say that the use of the deformable roll stabilizes the coating process and delays the onset of ribbing instability [47]. Scientists performed an experimental study of how operating parameters and the physical properties of the deformable roll cover influence the onset of ribbing instabilities, and could not find a regime that at negative gap would provide a stable coating [48]. However, the load increase, reduces the rib wavelength [49]. Studies (including experimental ones) of high speed roll to roll coating found that the roll speed and the coating viscosity are the key factors for misting, ribbing

and orange peel instabilities, which was showed in the multiple studies of Ascanio researcher [50, 51, 52]. A good experimental research of ribbing instabilities at high speed, was performed by Sasaki [53]. Also, Han studied experimentally the effect of fluid viscoelasticity in coating stability [54].

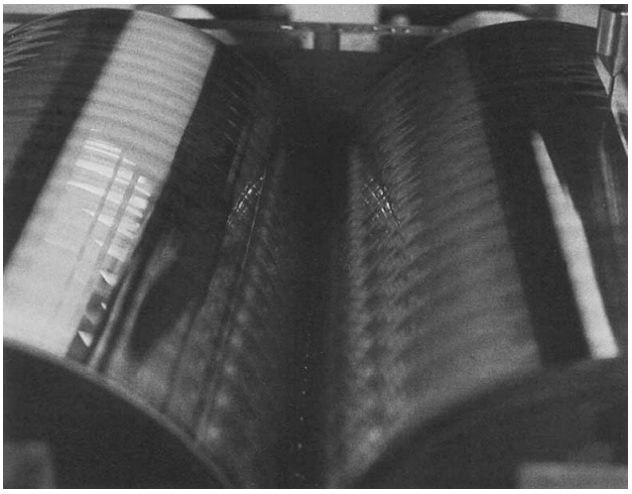

Figure 2.3: the photo of the ribbing instabilities during the forward roll coating

2.5 Experimental research in roll to roll coating

Besides Sasaki, Ascenio, Chong and Benkreira, many other scientists have performed the experimental research or roll to roll coating [55, 56]. Cohu performed experiments on the deformable forward roll coating of Newtonian fluids to observe how cover thickness, external load and roll speeds-ratio affect the coating thickness [57, 58]. To estimate the film thickness, the back-up roll simulated the web and the coating was scrapped off and weighted after the known period of time [57]. Gaskell investigated the meniscus using optical sectioning combined with dye injection and particle imaging techniques as well as measured the film thickness and compared with the existing theoretical data [59].

Experimental data from the mentioned studies were used by other scientists to validate their analytical and computational roll to roll studies. As already mentioned, Grashof did his study of influencing parameters based on analytical solution [5]. Willinger has also developed an analytical prediction for forward roll coating with deformable roll [4].

2.6 Latest work on the roll to roll coating

In the last 10 years, existing software provided more opportunities for computational research. Lucuyer has used Galerkin finite element method utilizing COMSOL and Matlab to obtain the

solution for Navier-Stokes equations and showed great simulation results [14] solving a coupled problem for the deformable forward roll coating with non-Newtonian fluids. There are also works performed in Ansys using the Volume of Fluid (VOF) method, for example, Chien and Jang got $15 - 20\%$ agreement of their simulation results with the experimental results for their study of reverse rigid roll coating with non-Newtonian fluids [60]. Another work done in Ansys with VOF model is presented by Kim, who was studying the printing ink transfer [42]. Even though, this work is not directly related, one can advise the approaches used to solve the similar problem in Ansys.

As one could notice, there is a gap, because nobody has done numerical simulation of the reverse roll coating problem with deformable rolls and non-Newtonian fluids. Also, very few works are industry oriented, like Lecuyer research [14]. However, there is a great work done by the FMP Technology Company together with AG Demmel Company published in summer 2020 [6]. They used the analytical approach to develop a software FMP-RRC-Program that provides "coating window" for parameters that are to be used for the stable coating in the reverse roll coating. Their goal is the digitalization and automation of the industrial coating processes. Even thought, the published work is for roll to roll coating, FPT Technology currently mainly specializes on the slot die coatings.

Chapter 3

Our system analysis

This research is oriented towards the specific system, so we have restricted geometry as well as some other operational conditions and parameters. The system geometry, conditions and parameters are taken from the real roll to roll coating system at NLMK coating shop floor. In their manufacturing, they use deformable roll systems to apply coating to the steel sheet that is later used for the household appliances. The coating is applied in two layers prime coating and enamel coating (paint coating). On NLMK plant, the steel sheet undergoes a full cycle shown in figure 1.1.

Usually, the reverse roll coating is used for the front side enamel paint applications, because it can provide thinner and more stable coatings, while forward roll coating used for the back side coating applications, where the one can sacrifice the quality. Deformable rolls are wearing off quickly, especially at reverse roll coating applications. Since the precision and stability, for the front side are more important, new deformable rolls are used only at reverse roll coating, after they have some degree of wear, they are transferred to the forward roll coating system for the prime coating application. However, sometimes the forward roll coating could be used at all the steps of the coating, as we will observe in the example.

3.1 NLMK roll to roll coating unit system description

The system consists of three rolls, as shown on figure 2.1. Roll 2 is a pick-up steel roll and its purpose it to take the paint, from the pan (marked with 1) and transfer it to the applicator roll (marked 3). The diameter of the metering roll is from 270 mm to 300 mm. The applicator roll has the 250 mm – 275 mm steel core rod covered with the polyurethane cover with the thickness of 30 mm. The polyurethane has the shore A hardness. The support roll (marked with 4), is a rigid steel roll with the diameter of 800 mm to 1000 mm. The steel sheet is moving between the applicator and support roll (marked with 5), and has the thickness from 0.3 mm to 0.8 mm. The picture of the system, similar to the one set in NLMK plant is shown in figure 3.1.

The speed of the web is form 40 m/min to 130 m/min and the support roll is rotated by means of the moving web. The metering and applicator roll speeds are up to 200% of the web speed that creates the slipping which helps to achieve a thin coating thickness. Big differences in the roll and line speeds, lead to the fast deformable cover wear off. Therefore, it is good to find

Figure 3.1: the picture of the whole roll to roll system with the pan fed setup

optimal parameters that could also help to extend the life of the deformable roll cover. The coating is applied to the both sides of the sheet. The coating thickness on the front side is approximately 25 μm, from which 5 μm is a prime coating and the rest 20 μm is an enamel coating.

On the manufacturing plant there are three systems. One works with the preset gap that is manually set by the operator. Two other systems, are newer and there the operator can automatically set the load between the applicator roll and support roll, as well as between the metering roll and applicator roll. Our research will be focused on the modeling the pre-set load case.

3.2 NLMK roll to roll coating system data analysis

We have received data from the NLMK Company (from date 01.03.12) to have an understanding of how the real operating parameters look like. Data was provided in the xls format in 3 files (enamel coating thickness measurements, prime coating thickness measurements, technical parameters data), as well as the legend for the technical parameters data column names, that was provided in email.

The whole system data analysis was performed in python Jupyter notebook via the pandas and matplotlib libraries. For technical parameters data frame, the column names were changed according to the provided legend. In raw data, the time was set in terms of current time. For the plotting needs the time was converted to the tracking time in and the first data point is set to 0. There are over 80000 seconds, therefore it was chosen to plot data points versus time in hours. There are about 25 hours of data collected.

In the provided technical parameters there are data for the 3 coating stations: prime coating station, 1^{st} enamel coating station and 2^{nd} enamel coating station. For the prime coating and 2^{nd} enamel coating stations we have data for both front and reverse side coating operations, while for the 1st enamel coating station we have only front side operational data. The steel sheet goes through all the stations. As one will see in figures 3.5 and 3.6, the enamel on the front side is applied in the first time period in the 1^{st} station, then at 14^{th} hour the enamel starts to be applies at the 2^{nd}

station.

For the prime coating front side we have data for applicator roll, pick-up roll and metering roll forces and velocities. However, the velocity of the metering roll in the current run is zero, therefore we can assume that it was not used at the moment when data was taken. In figure 3.2, one can observe four plot for the operational parameters of prime coating front side. As one can expect, applicator and pick up roll velocities are linear dependent. Also, since their velocities have opposite signs, we can say that we look at the forward roll coating. The applicator nip force is held constant at 4 kN, while the pick-up roll nip force has values of 4, 5 and 6 kN. The applicator roll velocity is from 55 to 65 m/min, and the pick-up roll velocity is from -30 to -40 m/min.

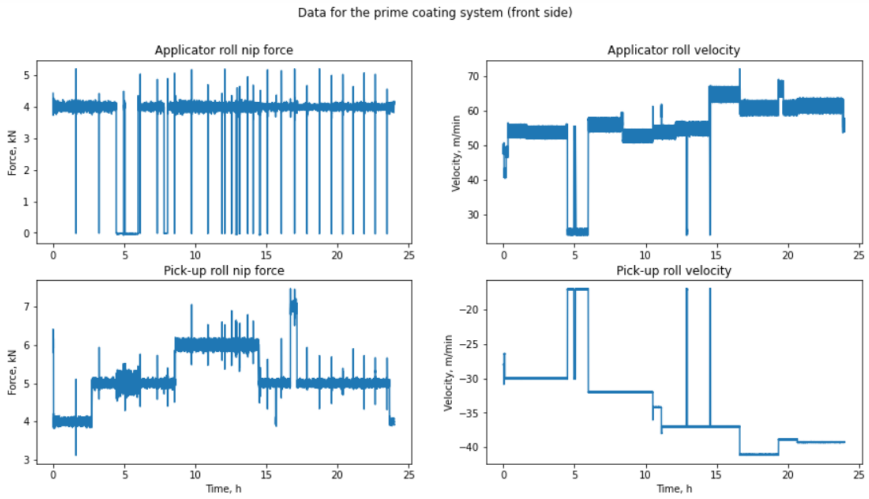

Figure 3.2: data for the prime coating system (front side) on 01.02.12

For the prime coating reverse side we have similar set of data, except that for the applicator roll is controlled not with the pre-set force way, but with the pre-set gap way, which we can observe on figure 3.3. Also, there are no data about the metering roll, because it is not used for the reverse sides of the sheet. The applicator roll gap is held constant at 1.30 mm and the velocity is about 50 m/min. The pick-up roll force has big variations from 4 to 14 kN.

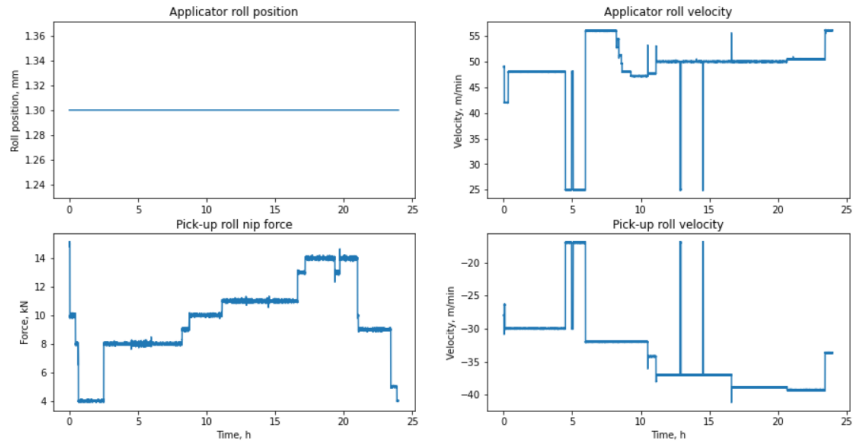

Figure 3.3: data for the prime coating system (reverse side) on 01.02.12

The prime coating data thickness measurements are shown in figure 3.4. We have average, minimum and maximum measurement data for both front and back side. By looking at the minimum and maximum measurements, one can see that that the uncertainty of the measurement is very big, especially for the reverse side measurements. Therefore, one could make a conclusion that prime coating material is hard for the measurement instrument. However, the prime coating measurement precision, is not as important as the precision for the enamel coating measurement, because the prime coating is cheap, comparing to the enamel coating used. The front side thickness is roughly constant and stays on about 6 μm. While the reverse side thickness decreases; it has started from 8 μm average thickness and dropped to the 6 μm.

Comparing plots in figures 3.3 and 3.4, we can observe a correlation for the reverse side coating. Even though the applicator roll position and velocity are held constant, the coating thickness decreases. However, this decrease correlates with the increase of the force nip and decrease of the velocity on the pick-up roll. We observe, what we would expect to observe, with the increase of force and velocity, the thickness layer becomes thinner.

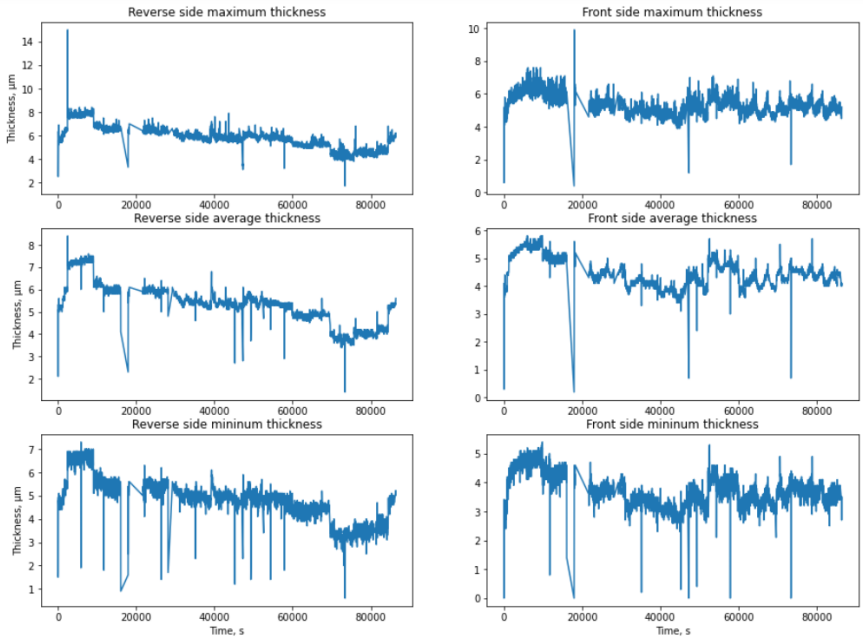

Figure 3.4: prime coating thickness measurements data on 01.02.12

As mentioned before, for the front side application two stations were used at different time period. The data for both stations is shown in figures 3.5 and 3.6. The applicator force stays within 5 to 6 kN, and the velocity of the applicator roll (at the periods, when the force is applied) is steadily increasing from 100 m/min to 140 m/min. The pick-up roll force is fairly constant at 10 kN in the first time period, and on the 2^{nd} station the force is more fluctuating with the average value of 13-14 kN. The velocity of the pick-up roll stays on 100 – 110 m/min.

The thickness measurements for the enamel are represented in figure 3.7. The measurements, are very precise, especially if compared (with eyes) with the prime coating thickness mea-

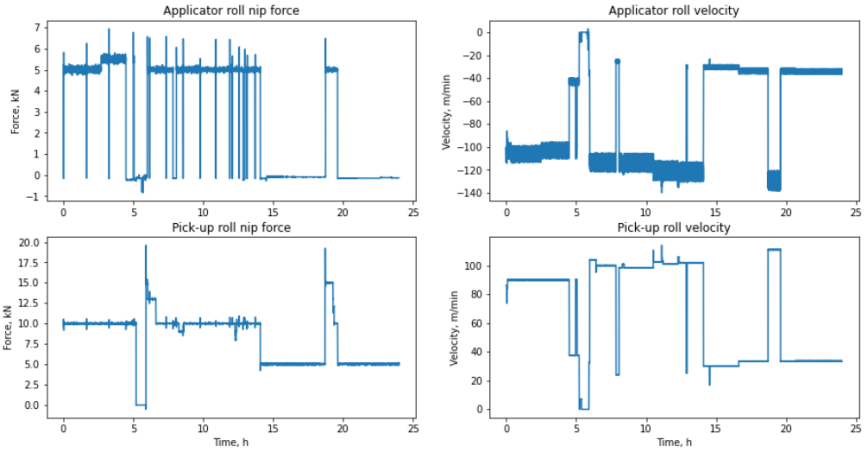

Figure 3.5: Operational data for the first painting station (front side) on 01.02.12

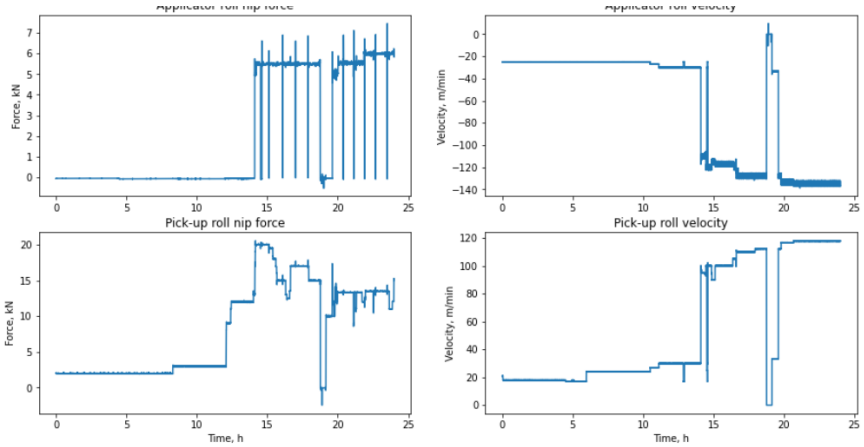

Figure 3.6: Operational data for the second painting station (front side) on 01.02.12

surements. On the reverse side the thickness is about 8 μm , while on the front side there is 20 μm, which is what we expected from the literature.

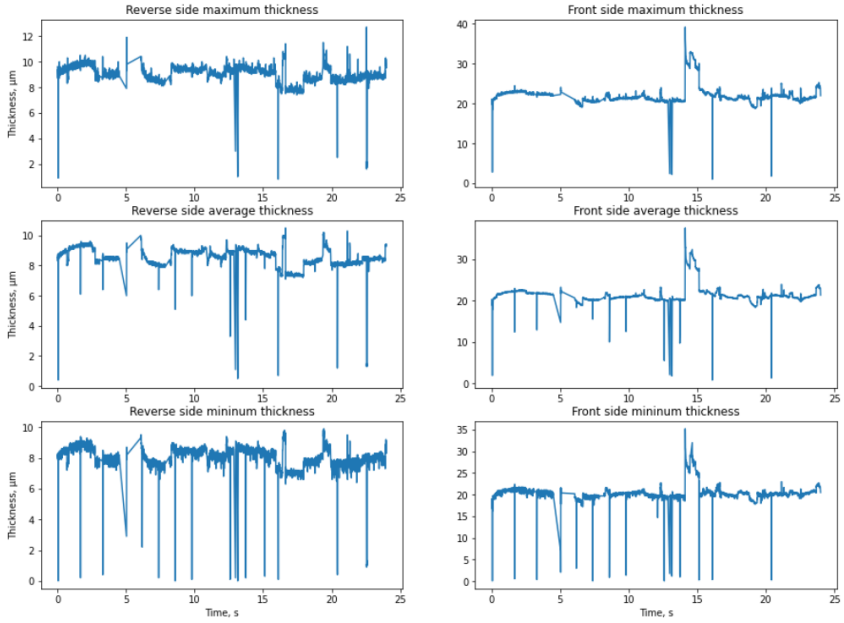

Figure 3.7: Enamel coating thickness measurements data on 01.02.12

Chapter 4

Methodology

The model is built via CFD (Computational Fluid Dynamics) and FE (Finite Element) modeling in commercial software ANSYS Fluent and ANSYS Structural 18.2. The methodology of this work consists of creating the numerical mechanical model for the elastomer of the applicator roll deformation and numerical model of the fluid flow simulation at the nip region. Then these models are joined together to create a coupled model that represents the deformavle roll to roll system.

4.1 Model selection for the elastomer

We performed the separate study of the mechanical model, to choose the appropriate model for the simulation of the elastomer. The model and its coefficients was chosen based on the experimental data, provided by the NLMK company. The study was performed by my colleague Alexander, therefore I will not go deeply into the details.

4.1.1 Geometry and mesh

The geometry is created via the design modeler that is build in in Ansys. For the mechanical part modeling, ¼ of the applicator roll geometry was taken. This is enough, because the deformation impact does not affect regions further out, as one can see in figure 4.1. Since, the experimental data, with the current results were compared, were collected, when the elastomer was pressed on the flat surface, the study for the elastomer model selection was performed in the similar conditions. The radius of the analyzed geometry was 170 mm, from where 30mm is the thickness of the elastomer.

For the following problem, the quadratic mesh was chosen, as shown in figure **??**. At the area of the deformation (the contact area) the mesh was refined, to ensure the precise calculations.

4.1.2 Model selection approach

In Ansys we set boundary condition such as bonded interaction between the elastomer and steel roll, and …..... between the roll and the surface. The force is set to be applied to the middle of the roll towards the surface. We obtain the deformation of the elastomer as the output parameter.

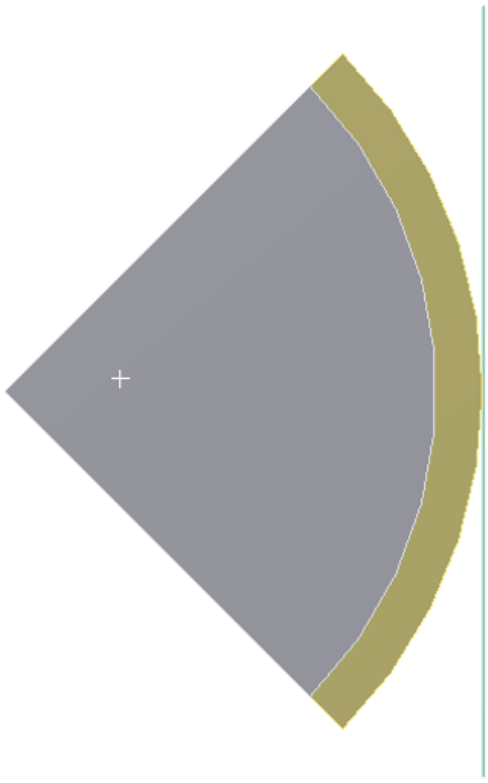

Figure 4.1: The geometry for the mechanical research of the elastomer

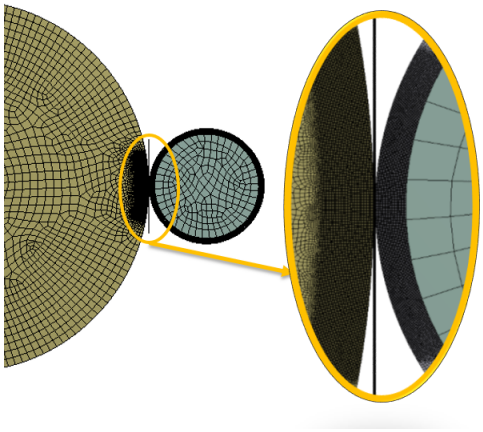

Figure 4.2: The mesh for the mechanical study of the elastomer

To choose the optimal model for the material and identification of its parameters, the provided experimental data was analyzed. The following function was created:

$$N = \sum_{i=1}^{n} \left[F_{Ex}\left(x_i\right) - F_{Th}\left(x_i\right) \right]^2 \tag{4.1}$$

where $F_{Ex}\left(x_i\right)$ and $F_{Th}\left(x_i\right)$ are experimental and theoretical magnitude of the force on the roll required to have the deformation x_i. With this function we analyze, which model gives the closest results to the real experimental values. For both models, Mooney-Rivlin and Blatz-Ko, were analyzed and the best parameters were chosen via optimization performed in pSeven software.

4.2 Fluid domain setup

The fluid part of the model was set up and studied separately for the multiple reasons. First, we had to research and practice working with the multiphase model (find the setup and BC parameters). Second, we had to choose model and coefficients for the non-Newtonian model. This study is crucial for this work, because all the parameters that were chosen here, were used for the coupled model.

4.2.1 Domain selection and geometry

The geometry is created via the design modeler in Ansys. For the fluid, the domain around the nip region was taken into account, as shown in figure **??**. Even though, the paint comes from the pad, we simulate the paint coming in through the input boundary condition. Solving the whole geometry would be computationally expansive and might not even be possible with the current computational resources.

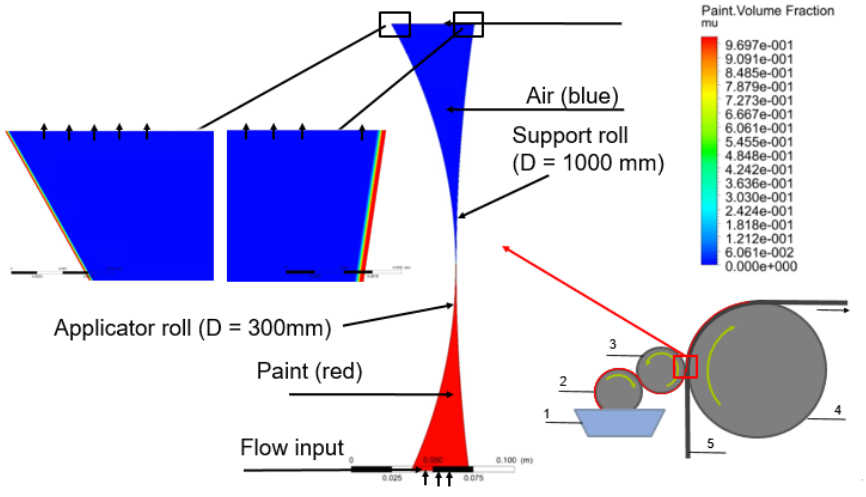

Figure 4.3: The fluid domain graphical representation

The geometry sizes for this study were chosen so that they are within the range of the provided sizes from NLMK. Therefore, the research is done on the real world size geometry. The support roll diameter is 1000mm and the applicator roll diameter is 300mm. The distance set between the rolls is 2mm.

4.2.2 Mesh

Mesh generation is one of the most important steps, because we need to create a mesh that will make our calculations robust without the loses in the accuracy of our model. Our fluid domain has several areas of interest, where most changes occur. First are is the nip region, which is the most

narrow region between the rolls. There fluid is a subject of the intense impact from both rolls. The same region has high impact from both rolls at the same time. As we go to the wider region, at some we start having less impact at the same area. The more impact we have – the finer mesh we have to make to keep the accuracy.

Therefore out domain is split into several regions, as one can observe on figure 4.4, where different parameters for the mesh size are applied. The value for the smallest size of the mesh was chosen based on the narrowest region. Also, the highest impact in general is at the wall, where the no slip BC is applied. There we also want to keep fine mesh, therefore the inflation parameter was used at the roll walls. Total we have 104487 nodes and 102373 elements.

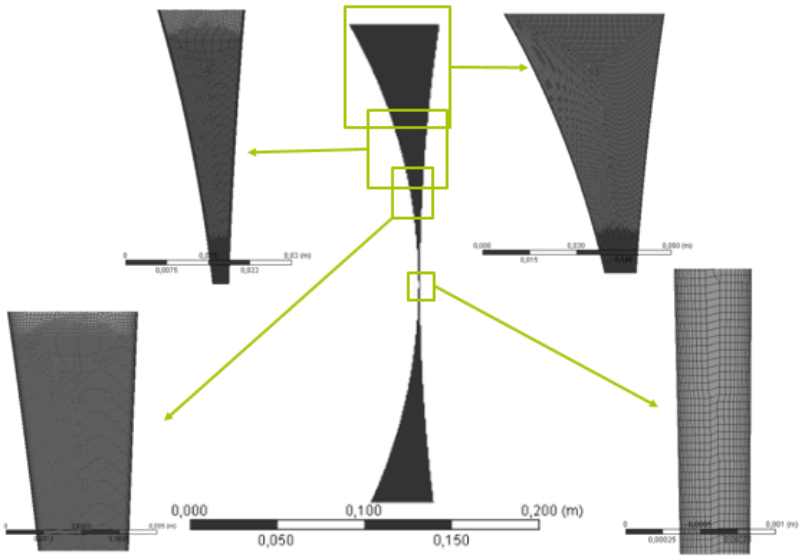

Figure 4.4: Mesh representation of the fluid domain for the fluid research

4.2.3 Model setup

For the research, two setups were used. For the first step, we aimed at setting up the multiphase model. While going through this setup, we will touch on many aspects that are the same for all the further setups.

First we look at the general setup window (see figure 4.5), where we choose pressure-based solver, with absolute velocity formulation. Our calculations are transient, because for the sake of research we are interested in what happens with the model at the moment of time. Also the nip region is very sensitive and there we choose a small time step, to make sure our calculation is complete. Gravity is neglected, because here it does not make any difference, which was discovered through the case of experiments.

Next, we choose the model, which in our case is a multiphase model called VOF (Volume of Fluid). According to literature research, this model is considered as the best choice for these

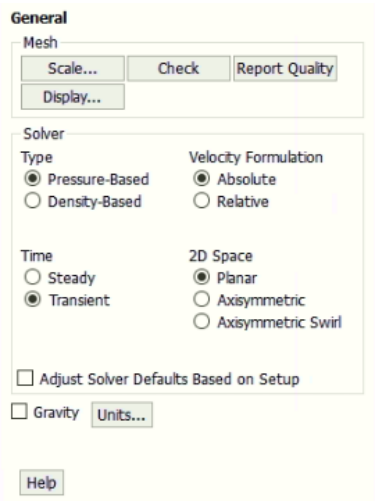

Figure 4.5: General settings in Ansys fluent

types of problems. On figure 4.6 we can look at the VOF model setup window. Here it is important to say, that we use explicit formulation and we have two Euclerian phases (those will be paint and air). For the phases we also set phase interaction with the surface tension coefficient 0.3 N/m. In the model, the paint is set as a primary phase and air - as a secondary phase.

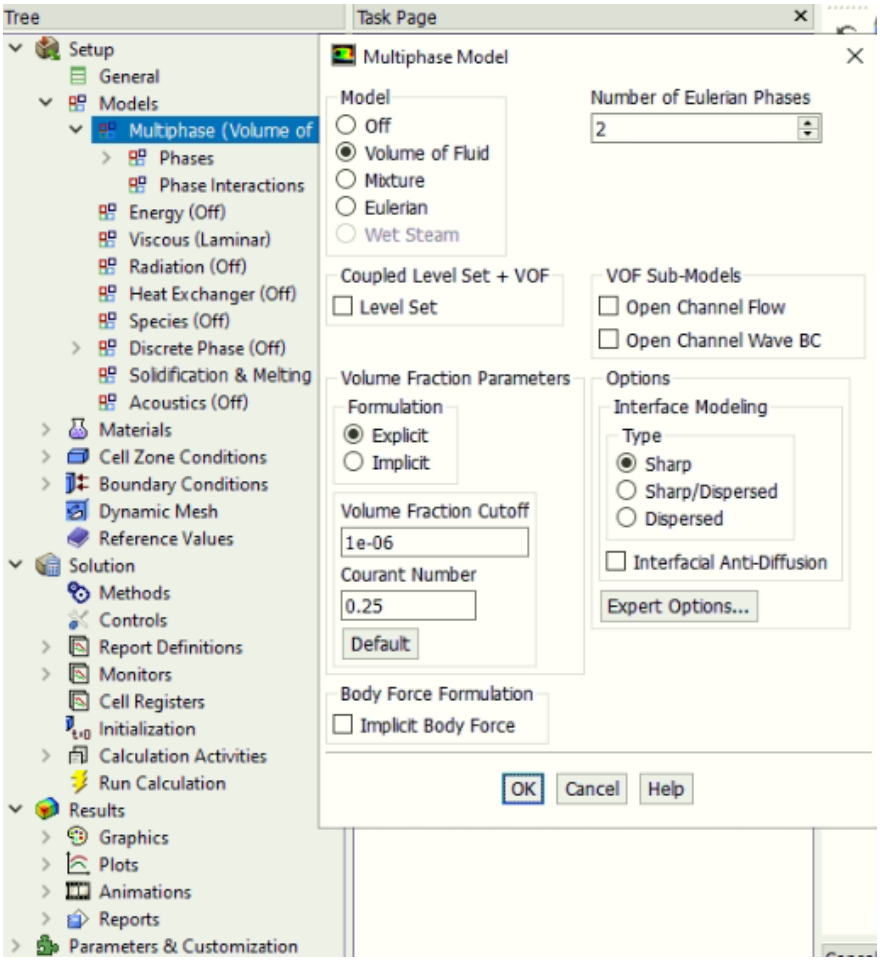

Figure 4.6: Multiphase model setup window in Ansys fluent

For the materials we create two fluids. For air we choose the properties from the library. For paint, density is set to 1280 kg/m3 and viscosity to 1.2 kg/m*s. In the material selection, this is where we use the non-Newtonian model. The power law model was used for the fluid and to set it up we need the consistency index and power law index, which depend on the fluid that is behind described by the model. To get the model coefficient for our fluids, we performed the power fit on the experimental data of paint provided by NLMK. The fit is performed with the inbuilt function in Maple software. Obtained coefficients are used in the model as shown in figure 4.7.

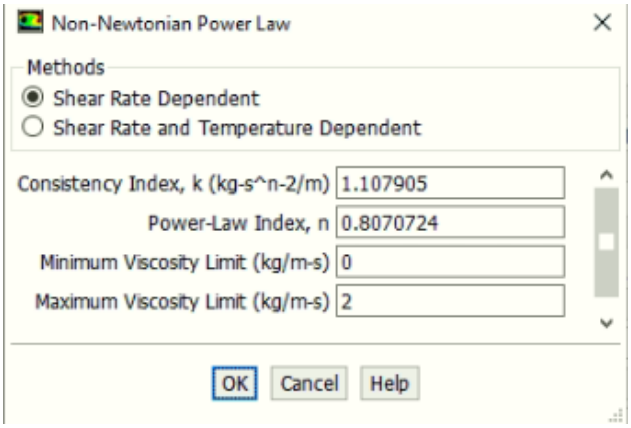

Figure 4.7: The non-Newtonian fluid model setup window in Ansys fluent

The boundary condition for the domain are shown also on figure 4.3. We have inlet on the bottom that is set as the velocity inlet. There we are imitating the paint flow that is coming from the rotating applicator roll. Inlet is set starting from 0.0048 m/s. The number was calculated based on the approximated expected output. We know approximate thickness and velocities of the roll. This way we calculate some outlet to get some degree numbers. We set inlet to the same degree as roughly expected outlet. This prevents our model from overflow of the paint, or the situation when there is not enough paint. The outlet is set to pressure outlet of gauge pressure equal to 0. The rolls boundary condition is treated as rotating walls with no slip condition. Rotation is set in rad/s and goes from 1 to 3.5 rad/s in our experiments. Applicator roll has positive rotation (counterclockwise), while the support roll has negative rotation (clockwise).

In methods section, the methods described in the literature review are used. The methods were chosen based on the literature research, best practices for thin coating simulation document, Ansys Fluent theory and users guide [43, 44, 45]. The methods window is shown in figure 4.8.The PISO pressure-velocity coupling scheme was chosen, with PRESTO! spatial discretization for pressure, Second order upwind for momentum and Geo-Reconstruct for volume fraction interface. Also the first order implicit transient formulation is used. In addition, in controls, the momentum is set to me 0.01, compared to the 0.7 that was recommended [43], because that allowed the computations to happen in our setup.

For the model we set the reports and plot to monitor mass flow at the outlet that is used to

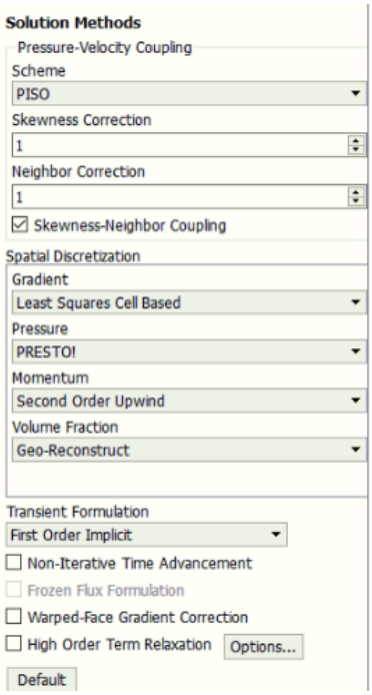

Figure 4.8: Methods window with chosen methods in Ansys fluent

see when then calculation is stable, as will be discussed in the results section. Initialization part here is also very important. We initialize the solution with zero velocities and air volume fraction set to 1. Then we mark the region that will be filled with paint and patch that region. That is our initial state, when the roll starts to rotate, we have half of the domain filled with paint. For the calculation we have to set the time step to $3 * 10^{-5}$ s with 20000 to 30000 steps. Such a calculation takes 4-5 hours.

4.2.4 Thickness measurement setup

To automate the thickness measurement the python script in the Ansys Workbench is used. Via the script we load the results for the volume fraction in each cell. We choose the region near the outlet, and set X_{start} and X_{max} values, where the X_{max} is the far right of the domain - the support roll wall. The representation of the region that we look at is at figure 4.9, where blue color represents air and red - paint. Everything in between is the interface. We divide the region in N segments and sample out at every step the volume fraction. Once the volume fraction is greater than 0.5, we denote that place with X. The thickness is calculated by $X_{max} - X$. The scrips is can be found in Appendix (.....)

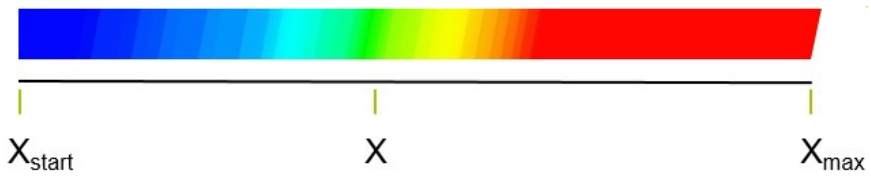

Figure 4.9: Representation of the automatic thickness measurement

4.3 Coupled model

Coupled model implementation also happens in Ansys software via the special coupled model interface. To do so, we have to create a geometry that has both solid and fluid domains and setup fluid solver for the fluid domain and transient structural solver for the solid domain. The whole setup architecture is shown in figure 4.10. One of the main difficulties that there is in the coupled model, is that we have to make a 3 dimensional model in order to create the coupled system. Therefore, the time that is required for the calculation has increased drastically.

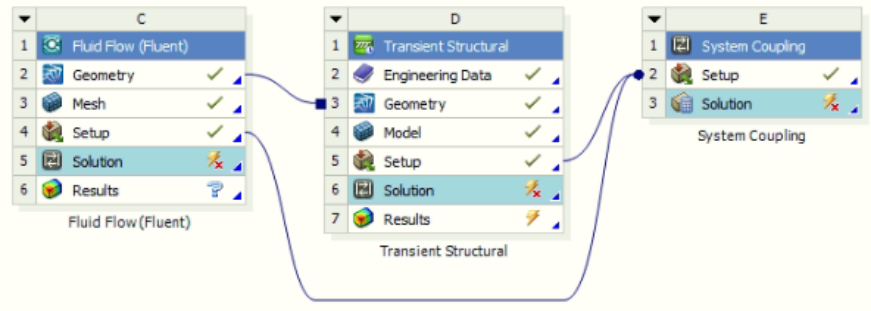

Figure 4.10: Coupled model setup in Ansys workbench

4.3.1 Geometry

The geometry for the coupled model is the connection of the geometries discussed in the mechanical and fluid sections of this work, and it is shown in figure 4.11. It was chosen that the radius of the support roll is 400 mm, and the radius of the applicator roll is 150 mm, from where 30 mm is the elastomer. We set 3 mm gap between the rolls. Since we need a 3D geometry, the thickness was set to 1mm We could not choose smaller thickness, because otherwise the mechanical calculations were not converging.

4.3.2 Mesh

4.3.3 Model setup

We use the applicator wall as the fluid solid interface where the data between the solvers is being exchanged. Fluid solver provides the pressure data to the mechanical solver, while the mechanical

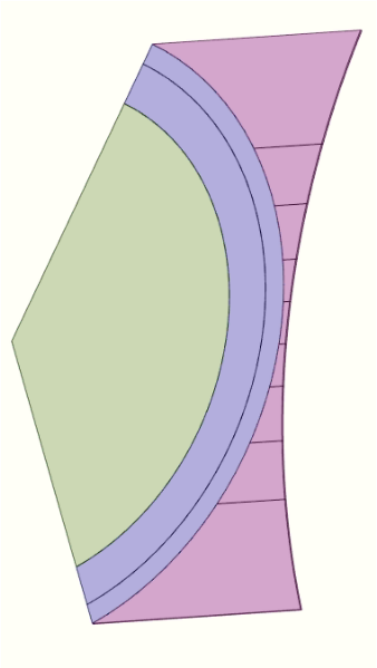

Figure 4.11: The full 3D geometry for the coupled system computations

solver provides the deformation data to the fluid domain. Data is being exchanged at every step, and the degree of deformation effects on that pressure will be given to the fluid, that affects the degree of deformation and so on. We are sensitive to every step, therefore we must perform the transient calculation. This is the model setup that is ready to go, and will be used in the further research calculations.

Chapter 5

Results

5.1 Elastomer choice research

As the results of the simulations we get the stress distribution as shown in figure 5.1 where one can also observe the shape deformation of the elastomer. One can see, that as expected, there is basically no deformation of the steel roll, just the outer elastomer is being deformed. As the output parameter we also get the deformation values that are used to be compared with the experimental results.

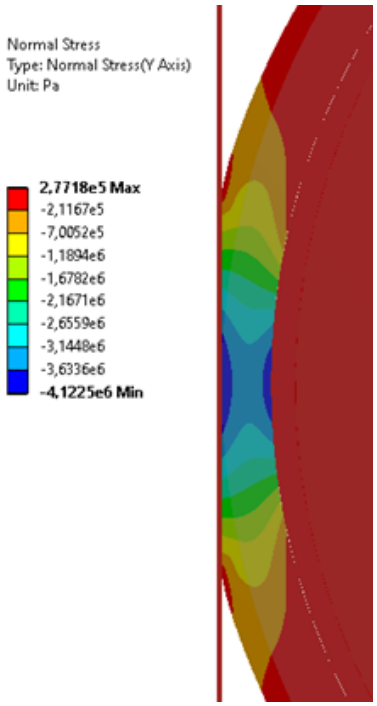

Figure 5.1: The normal stress distribution representation of the elastomer FE analysis

As mentioned before, for both Mooney-Rivlin and Blatz-Ko models to choose the parameters that would fit best the optimization run was performed in the pSeven software. Then with eq 4.1 we compare which model is closest to the experimental results, and Blatz-Ko model appeard to shoe better results than Mooney-Rivlin. The data points comparison plot is shown in figure 5.2. One can observe that experimental data looks not uniform, which brings in the degree of error. NLMK, who did the experiment, said that it was just a testing experiment and promised to per-

form better experiments with more data, so we could build a more precise model. At this point, using this study, the Blatz-Ko model with the pSeven defined parameters is chosen for the further experiments of this research.

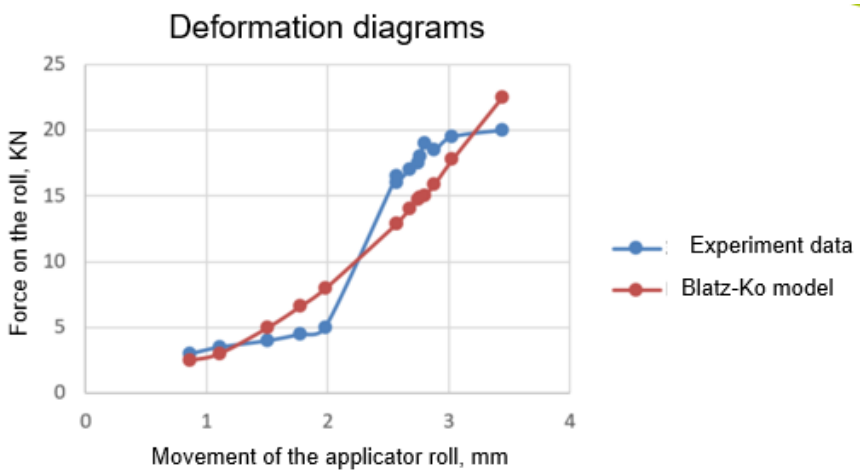

Figure 5.2: The comparison of the results for the Blatz-Ko model with the experimental data for the elastomer analysis

5.2 2D fluid flow analysis

The fluid flow calculations are much harder to implement and they take more computational power than the mechanical studies. As mentioned before, one calculation takes up to 5 hours. In the early stages of my research, this calculation was taking 30 hours, but we managed to optimize it.

The calculation is transient, and we had to decide when do we stop the calculation. We are plotting the mass flow rate at the outlet as a function of time, as shown in figure 5.3. This value shows us how much paint it going through the outlet at the moment of time. This value is directly correlates with the paint thickness on the rolls. It is important to note that one roll is faster than the other one (there are different setting that were tested), therefore at some point we have mass flow rate that is paint from just one roll, and at some point there is paint from both walls. As we can wee on the plot, the mass flow rate fluctuates, this means that thickness is not stable yet, and we were able to observe it on the contour plot. At some point, near the first second of our calculations, the mass flow rate stabilizes at one constant value. This means that the paint thickness at both rolls is stable. Once the stability is reached, we stop our calculations.

The representation of the contour plot was already shown in figure 4.3 in the setup section of this work. For us, the most important region to look at is the outlet region at the walls. There we can see the paint thickness far away from the nip, which would be the same thickness that stays on the steel sheet after it is coated. The enlarged region of the outlet on the support roll is shown in figure 5.4. On the shown figure, one can see that the thickness of the current example is roughtly

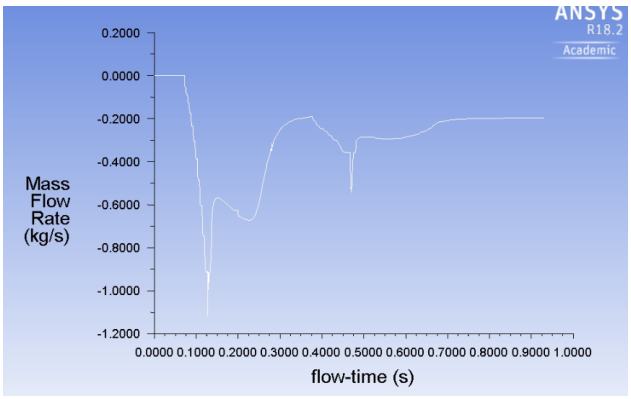

Figure 5.3: The plot of mass flow rate versus time for the fluid flow calculations in Ansys

0.000091 m = 91 μm. This result was obtained with the support roll speed 1.4 radand the applicator roll speed 1 radfor the regular Newtonian fluid.

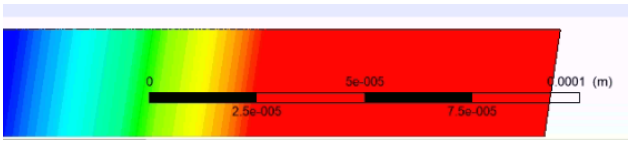

Figure 5.4: The enlarged area of the output on the support roll, where the paint thickness can be observed

5.2.1 Regular fluid results

For the regular fluid, we have conducted 5 complete runs and the results are accumulated in table 5.1. All runs were performed with the constant applicator roll speed that was set to 1 rad. Looking at the data, one can notice that the applicator roll thickness stays more or less stable, while the support toll thickness changes linearly.

Table 5.1: the segmentation of the roll coating systems

Support roll (rad/s)	Applicator roll thickness (m)	Support roll thickness (m)	Time steps	Mass flow output (kg/s)	Mass flow input (kg/s)
1.4	5.7e − 005	**9.10E − 04**	26000	−0.187039	0.182261
1.5	4.7e − 005	**9.30E − 04**	31004	−0.197878	0.195931
1.6	4.5e − 005	**9.50E − 04**	33435	−0.211327	0.2096
1.7	4.5e − 005	**9.70E − 04**	28420	−0.229579	0.227826
1.8	4.6e − 005	**1.00E − 03**	30501	−0.245842	0.243774

We have plotted the support roll thickness as a function of support roll velocity and indeed we see the linear dependency, shown in figure 5.5. It is interesting, that the faster the roll is rotating, the more paint stays on it, what increases the thickness of the coating.

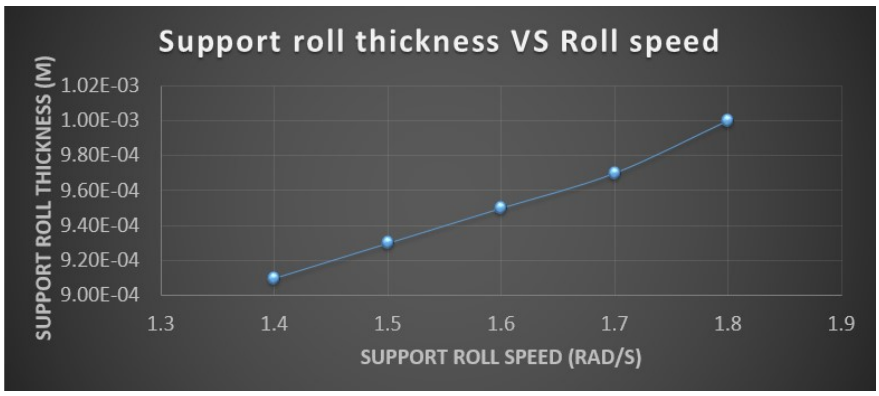

Figure 5.5: The plot of the support roll thickness as a function of the support roll speed

5.2.2 Non-Newtonian fluid results

Non-Newtonian fluid calculations were performed also with the different input parameters. We have studied how coating thickness depends on the changes in the applicator roll speed, as well as, on the distance between the rolls. Before looking at the results, we want to show the non-Newtonian fluid properties in action. In figure 5.6 we show the viscosity contour plot of the domain. Red colors represent low viscosity regions, and blue are high viscosity regions. As the rolls are rotating, the fluid in near the walls is a subject to the high shear stress. In the middle of the bottom part of the domain, we have region of high viscosity, because fluid there is not subject to any shear stress. In the most narrow region we have the area of the lowest viscosity, because there the fluid gets the highers shear stress values, as they are coming closely from both rolls. However, when we go further out, to the areas where the coating just sits on the roll, the viscosity gets higher. The interaction of paint with air is low and air does not provide much shear stress on the boundary to the paint. With the wall paint has no slip condition. Since air does not hold the paint in place it freely moves along with the roll. Basically the paint is drying out on the roll.

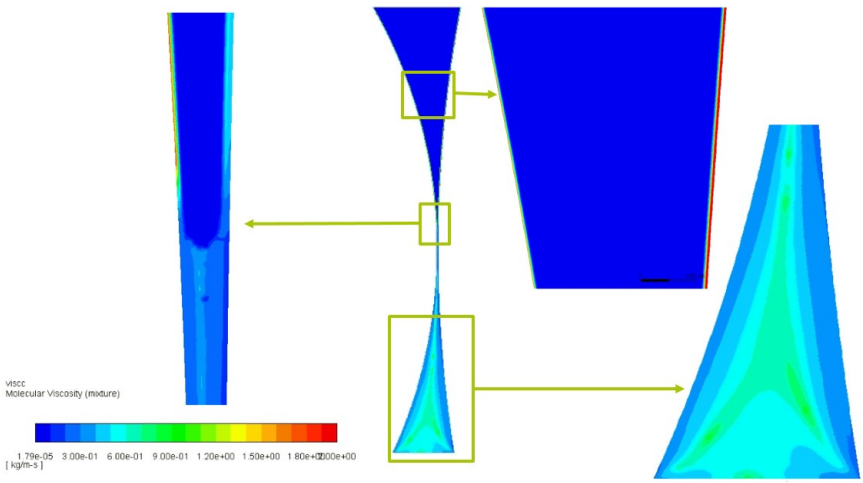

Figure 5.6: The viscosity contour plot of the calculation for the roll to roll coating on the non-Newtonian liquid

As mentioned before, for the non-Newtonian liquid we have performed two studies. The results for the study of how the thickness depends on the applicator roll speed is shown in figure 5.7. Even though for us it is more important to look at the thickness of the support roll, there we show how the applicator roll thickness depends on the applicator roll velocity. The support roll velocity is kept constant. Unexpected for us, but the support toll thickness stayed constant (75μm). The applicator toll thickness is increasing as we increase the speed of the roll.

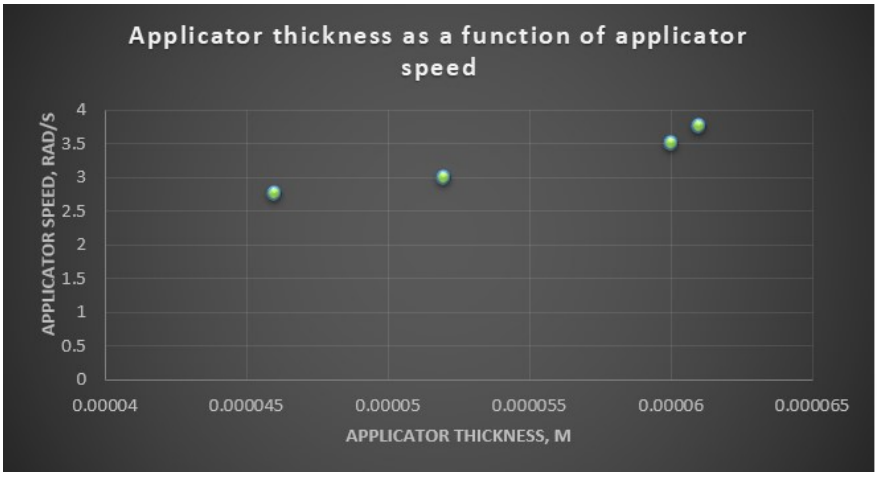

Figure 5.7: The plot of the applicator roll thickness as a function of the applicator roll speed for non-Newtonian liquid

Variating the distance between the rolls also did not affect the support roll thickness, however it did affect the applicator roll coating thickness. This dependency is represented in figure *. We observe that as we increase the separation thickness, the applicator roll thickness is decreasing, and there is an exponential dependency.

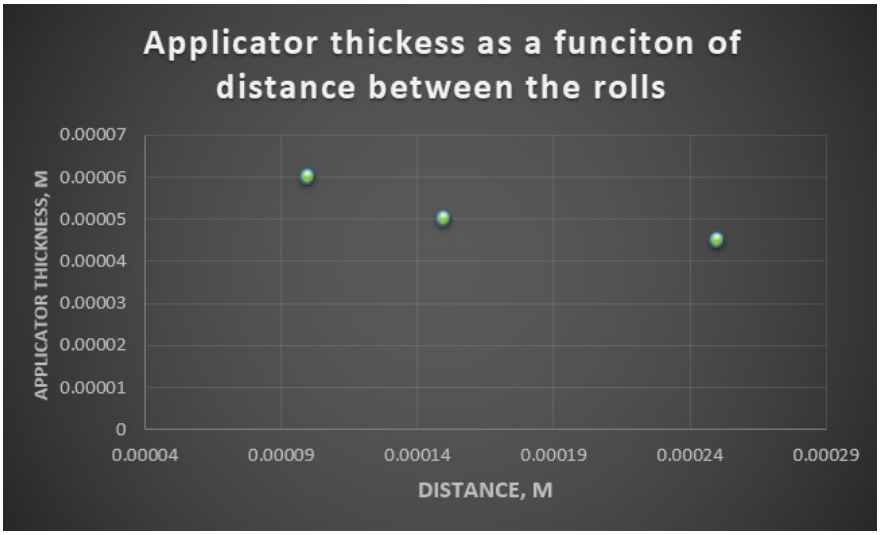

Figure 5.8: The plot of the applicator roll thickness as a function of separation roll distance for non-Newtonian liquid

5.3 Discussion

We have shown the results of the fluid analysis, which is the study of the rigid roll to roll coating simulation, to the NLMK expert. The expert said that the results are reasonable together with the dependencies that we have observed. The behavior of the non-Newtonian liquid discussed is physically real, which is a proof for us that the model is physically correct.

The results that we observed on when the velocity applicator roll was changing, showed that support roll thickness stayed constant. Here to point out, that when the support roll velocity was changes, the applicator roll speed also stayed close to constant (with few exceptions). That is an interesting observation, where we can say that the speed of specific roll affects the thickness on the roll, not their rations, as it was mentioned often in the literature. The ration, of course, than also is changing, but main correlation is within the specific data for specific roll. Another interesting correlation observed is that changing the distance between the rolls, only the applicator roll thickness has changed. This does not directly agree with the literature data, therefore this phenomenon must be research more and validated with experiments.

However, we cannot directly validate our results with some experimental values, because for rigid roll results we would have to build a completely new experimental setup, and in the scope of master thesis that was not planned. The experimental results in the literature have been performed on specific setups, mostly rigid rolls. In addition, some authors show results in terms of ratios, and because of that for me it was hard to validate the results properly. To make a proper verification, analytical calculations could be performed, which we have started, but not all papers provide detailed explanation and validation of their analytical research, which make the analytical calculation to be a much more time consuming task, so it stayed out of the scope for the master thesis. Finally, the validation could be performed on the real plant data on NLMK, however, it could be done only with the deformeable model (coupled model), which we have not received the results yet.

However, to make the model values close to the real world values, we have to compare them with the real world examples. To do so, we need to do the validation and it has to be done on the deformable roll to roll coating system that we are implementing via the coupled model.

5.3.1 Value of the results

This research is fundamental for the main goal of the project, which is a recommendation system for the roll to roll coating systems in NLMK. The literature research perfromed is a backbone of the project. Also, we have found a way to simulate and model the physical processes. The recommendation system architecture is shown in figure 5.9. The performed work in the scope of

this master thesis is hidden in the left side of the recommendation system architecture.

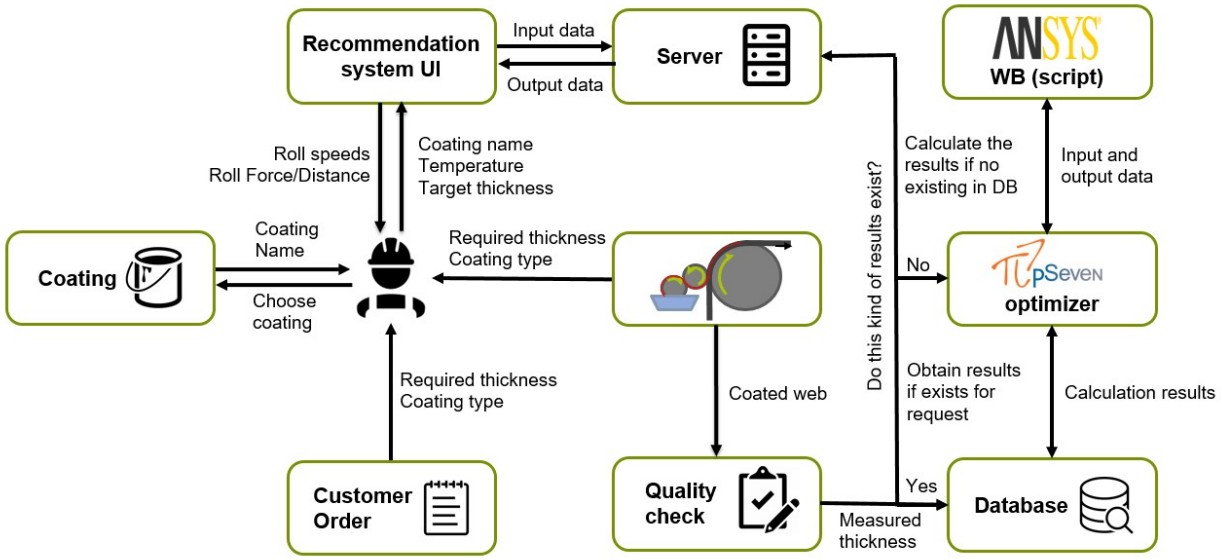

Figure 5.9: Architecture for the recommendation roll to roll coating system

All the performed work can be used to continue build on it to have the final model for deformable roll systems. We have ready hypotheses on how to improve and change the model to increase the accuracy of our results.

Besides the industrial application, the methods used in this research can be a step forwards in the research of the thick film application numerical computation area. Since, there was almost no modern research on this topic, this could be a good step up.

5.3.2 Possibilities for future development

This work is a first step of what could be done in the direction of the full recommendation system. Further the coupled model should be finished and generated many results that could be optimized and validated on the NLMK plant. In addition, this work focuses on the forward roll coating, therefore more data and research could be done on the reverse roll coating. The methods could be compared. Also, more models could be tested to solve this proble, for example the fluid film model that is build in Ansys, or we could try Star-CCM+ software to perfrom the calculation and verification of the results.

Also, the for the industrial and optimization purposes, the whole simulation could be written in the Ansys WB script, where we set input parameters such as roll speeds, applicator roll force and fluid properties, and receive support and applicator roll thicknesses. This script can be passes to the pSeven optimizator, which would be a ready to use scientific part of the recommendation system.

5.3.3 Potential impacts on innovation

This work has a potential to be a starting point for the automatization of the roll to roll coating processes. We are in the era of Industry 4.0 and digitalization is happening on all spheres of lives, including the manufacturing. First step of recommendation system, would be to give an operator suggestions which parameters to set on the apparatus, to get the desired coating thickness with the specific coating color. The next step involves, the in build system in the apparatus, where the operator just has to enter the coating color (all the coatings physical parameters used on the plant will be in build) and the desired thickness. The system will automatically set the parameters and automatically perform the calibration, based on the data received from the sensors installed.

Such studies are happening in Germany, on the government level with the leading companies in this sector but for a slot die systems. There are still plenty of manufacturing plants that are using roll to roll coating. Providing them a recommendation system solution, would be a cheaper way of their system automatization, that installing a whole new apparatus. The solution would save a lot of money for manufacturing plants.

Chapter 6

Conclusion

The central goal of this research was to develop a fundamental starting point for the recommendation system of the roll to roll coating industrial applications. The method to achieve the goal was the numerical simulation of the coating process in the Ansys 18.2 modeling software, where Anays Mechanical and Ansys Fluent was used.

The deeply research the literature and methods used in the last to decades to solve this kind of problem was performed. Also the provided measurements from the NLMK were analyzed and visualized on the plots using python and excel. Especially important was, to get the coefficients for the non-Newtonian fluid to be used in the model, from the provided experimental data. For the mechanical part, the experimental data of the elastomer were used to choose the best model and coefficients via the pSeven software. The domain, geometry, mesh and boundary conditions were chosen and developed. Through the research and experiments methods and models were chosen for the numerical computation. The results were obtained for the regular fluid and different support roll speeds, and for non-Newtonian fluid with different applicator roll speeds and different separation distances between the rolls. The work performed in the scope of the master thesis can be used to be further developed in the recommendation system.

Appendix A

Code

```
import os
import math
# encoding: utf-8
# Release 18.2
SetScriptVersion(Version="18.2.109")

pi=3.14159265358979323846264338327 95

dir='C:/Users/User/Documents/Arina/Skolkovo'

system1 = GetSystem(Name="FFF 2")
solution1 = system1.GetContainer(ComponentName="Solution")
solution1.Edit()

def ReadVoF(file,nCol):
  f = open(file)
  for i in range(nCol):
    f.readline()
  value=''
  line=f.readline()
  s=line[:(len(line)-1)]
  while (not ((s[len(s)-1]=='\t') or (s[len(s)-1]==' ')))and(len(s)>1):
    value=s[len(s)-1]+value
    s=s[:(len(s)-1)]
  if (len(s)==1) and (not ((s[len(s)-1]=='\t') or (s[len(s)-1]==' '))):
    value=s[0]+value
  return (float(value))

fileMaxY=dir+'/MaxY.dat'
f=open(fileMaxY,'w')
f.close()
solution1.SendCommand(Command='/report/surface-integrals/facet-max output ()
    mixture y-coordinate y '+fileMaxY)
y=ReadVoF(fileMaxY,5)
```

```
34
35 fileMinX=dir+'/MinX.dat'
36 f=open(fileMinX,'w')
37 f.close()
38 solution1.SendCommand(Command='/report/surface-integrals/facet-min output ()
       mixture x-coordinate y '+fileMinX)
39 xMin=ReadVoF(fileMinX,5)
40
41 fileMaxX=dir+'/MaxX.dat'
42 f=open(fileMaxX,'w')
43 f.close()
44 solution1.SendCommand(Command='/report/surface-integrals/facet-max output ()
       mixture x-coordinate y '+fileMaxX)
45 xMax=ReadVoF(fileMaxX,5)
46
47 x=xMax-(xMax-xMin)/100
48
49 nSegm=20
50 dx=(xMax-x)/nSegm
51 file=dir+'/newPoint.dat'
52 Find=False
53 d=0.0
54 i=0
55 while (not Find) and (x!=xMax):
56   f=open(file,'w')
57   i=i+1
58   solution1.SendCommand(Command='/surface/point-surface newPoint'+str(i)+' '+
       str(x)+' '+str(y))
59   solution1.SendCommand(Command='/report/surface-integrals/vertex-avg newPoint
       '+str(i)+' () paint vof y '+file)
60   VoF=ReadVoF(file,5)
61   if (VoF>0.0):
62     Find=True
63     d=abs(xMax-x)
64   else:
65     x=x+dx
66 file2=dir+'/PaintThickness.dat'
67 f=open(file2,'w')
68 f.write('Paint Thickness: '+str(d)+'\n')
69 f.close()
70 solution1.Exit()
```

Listing A.1: The script used in the Ansys workbench to automatically measure the film thickness on the support roll

Bibliography

[1] S. Sarma, "Fluid mechanics of high speed deformable roll coating. an experimental and theoretical study of film thickness and stability in high speed deformable roll coating flow with newtonian and non-newtonian liquids," Ph.D. dissertation, University of Bradford, 2015.

[2] S. Abbott, N. Kapur, P. Sleigh, J. Summers, and H. Thompson, "A review of deformable roll coating systems," *Convertech & e-Print*, vol. 1, no. 3, pp. 89–93, 2011.

[3] H. Benkreira, R. Patel, M. Edwards, and W. Wilkinson, "Classification and analyses of coating flows," *Journal of non-newtonian fluid mechanics*, vol. 54, pp. 437–447, 1994.

[4] B. Willinger and A. Delgado, "Analytical prediction of roll coating with counter-rotating deformable rolls," *Journal of Coatings Technology and Research*, vol. 11, no. 1, pp. 31–37, 2014.

[5] B. Grashof and A. Delgado, "Analysis of influencing parameters in deformable roll coating of counter-rotating rolls," *Journal of Coatings Technology and Research*, vol. 12, no. 1, pp. 63–73, 2015.

[6] G. Zheng, F. Wachter, A. Al-Zoubi, F. Durst, R. Taemmerich, M. Stietenroth, and P. Pircher, "Computations of coating windows for reverse roll coating of liquid films," *Journal of Coatings Technology and Research*, vol. 17, no. 4, pp. 897–910, 2020.

[7] S. F. Kistler and P. M. Schweizer, *Liquid film coating: scientific principles and their technological implications*. Springer, 1997.

[8] H. Benkreira, Y. Shibata, and K. Ito, "Thinnest uniform liquid films formed at the highest speeds with reverse roll coating," *AIChE Journal*, vol. 59, no. 8, pp. 3083–3091, 2013.

[9] M. Gostling, M. Savage, A. Young, and P. Gaskell, "A model for deformable roll coating with negative gaps and incompressible compliant layers," *Journal of Fluid Mechanics*, vol. 489, pp. 155–184, 2003.

[10] H. Benkreira, Y. Shibata, and K. Ito, "Reverse roll coating with a deformable roll operating at negative gaps," *Chemical Engineering Science*, vol. 165, pp. 204–215, 2017.

[11] G. Ascanio, P. Carreau, and P. Tanguy, "High-speed roll coating with complex rheology fluids," *Experiments in fluids*, vol. 40, no. 1, pp. 1–14, 2006.

[12] S. K. Han, D. M. Shin, H. Y. Park, H. W. Jung, and J. C. Hyun, "Effect of viscoelasticity on dynamics and stability in roll coatings," *The European Physical Journal Special Topics*, vol. 166, no. 1, pp. 107–110, 2009.

[13] G. Parish, "Measurements of pressure distribution between metal and rubber covered rollers," *British Journal of Applied Physics*, vol. 9, no. 4, p. 158, 1958.

[14] H. Lécuyer, J. Mmbaga, R. Hayes, F. Bertrand, and P. A. Tanguy, "Modelling of forward roll coating flows with a deformable roll: Application to non-newtonian industrial coating formulations," *Computers & Chemical Engineering*, vol. 33, no. 9, pp. 1427–1437, 2009.

[15] J. Mmbaga, R. Hayes, F. Bertrand, and P. Tanguy, "Flow simulation in the nip of a rigid forward roll coater," *International journal for numerical methods in fluids*, vol. 48, no. 10, pp. 1041–1066, 2005.

[16] D. Coyle, C. Macosko, and L. Scriven, "Computer simulation of nip flow in roll coating," 1982.

[17] D. Coyle, C. Macosko, and L. Scriven, "Film-splitting flows in forward roll coating," *Journal of Fluid Mechanics*, vol. 171, pp. 183–207, 1986.

[18] D. Coyle, C. Macosko, and L. Scriven, "Film-splitting flows of shear-thinning liquids in forward roll coating," *AIChE journal*, vol. 33, no. 5, pp. 741–746, 1987.

[19] D. Coyle, C. Macosko, and L. Scriven, "Stability of symmetric film-splitting between counter-rotating cylinders," *Journal of Fluid Mechanics*, vol. 216, pp. 437–458, 1990.

[20] D. Coyle, "Forward roll coating with deformable rolls: A simple one-dimensional elastohydrodynamic model," *Chemical engineering science*, vol. 43, no. 10, pp. 2673–2684, 1988.

[21] D. Coyle, C. Macosko, and L. Scriven, "The fluid dynamics of reverse roll coating," *AIChE Journal*, vol. 36, no. 2, pp. 161–174, 1990.

[22] D. Coyle, C. Macosko, and L. Scriven, "The fluid dynamics of reverse roll coating," *AIChE Journal*, vol. 36, no. 2, pp. 161–174, 1990.

[23] D. J. Coyle, C. W. Macosko, and L. Scriven, "A simple model of reverse roll coating," *Industrial & engineering chemistry research*, vol. 29, no. 7, pp. 1416–1419, 1990.

[24] M. Carvalho and L. Scriven, "Deformable roll coating: Modeling of steady flow in gaps and nips," in *The Mechanics of Thin Film Coatings*. World Scientific, 1996, pp. 221–230.

[25] M. Carvalho and L. Scriven, "Three-dimensional stability analysis of free surface flows: application to forward deformable roll coating," *Journal of Computational Physics*, vol. 151, no. 2, pp. 534–562, 1999.

[26] M. S. Carvalho and L. Scriven, "Deformable roll coating flows: steady state and linear perturbation analysis," *Journal of Fluid Mechanics*, vol. 339, pp. 143–172, 1997.

[27] M. Carvalho, "Effect of thickness and viscoelastic properties of roll cover on deformable roll coating flows," *Chemical engineering science*, vol. 58, no. 19, pp. 4323–4333, 2003.

[28] M. Carvalho and L. Scriven, "Flows in forward deformable roll coating gaps: comparison between spring and plane-strain models of roll cover," *Journal of Computational Physics*, vol. 138, no. 2, pp. 449–479, 1997.

[29] H. Benkreira, M. Edwards, and W. Wilkinson, "A semi-empirical model of the forward roll coating flow of newtonian fluids," *Chemical Engineering Science*, vol. 36, no. 2, pp. 423–427, 1981.

[30] H. Benkreira, M. Edwards, and W. Wilkinson, "Roll coating of purely viscous liquids," *Chemical Engineering Science*, vol. 36, no. 2, pp. 429–434, 1981.

[31] H. Benkreira, M. Edwards, and W. Wilkinson, "Roll coating operations," *Journal of non-newtonian fluid mechanics*, vol. 14, pp. 377–389, 1984.

[32] H. Benkreira, Y. Shibata, and K. Ito, "Thinnest uniform liquid films formed at the highest speeds with reverse roll coating," *AIChE Journal*, vol. 59, no. 8, pp. 3083–3091, 2013.

[33] Y. Greener and S. Middleman, "A theory of roll coating of viscous and viscoelastic fluids," *Polymer Engineering & Science*, vol. 15, no. 1, pp. 1–10, 1975.

[34] N. Ali, H. M. Atif, M. A. Javed, and M. Sajid, "A theoretical analysis of roll-over-web coating of couple stress fluid," *Journal of Plastic Film & Sheeting*, vol. 34, no. 1, pp. 43–59, 2018.

[35] M. Zahid, T. Haroon, M. Rana, and A. Siddiqui, "Roll coating analysis of a third grade fluid," *Journal of Plastic Film & Sheeting*, vol. 33, no. 1, pp. 72–91, 2017.

[36] S. Khaliq and Z. Abbas, "A theoretical analysis of roll-over-web coating assessment of viscous nanofluid containing cu-water nanoparticles," *Journal of Plastic Film & Sheeting*, vol. 36, no. 1, pp. 55–75, 2020.

[37] S. Sofou and E. Mitsoulis, "Roll-over-web coating of pseudoplastic and viscoplastic sheets using the lubrication approximation," *Journal of Plastic Film & Sheeting*, vol. 21, no. 4, pp. 307–333, 2005.

[38] Y. Hao and S. Haber, "Reverse roll coating flow," *International journal for numerical methods in fluids*, vol. 30, no. 6, pp. 635–652, 1999.

[39] M. Chandio and M. Webster, "Numerical simulation for reverse roller-coating with free-surfaces," *press Int. J. Num. Meth. Heat Fluid Flow*, 2001.

[40] S. Echendu, H. Tamaddon-Jahromi, and M. Webster, "Modelling polymeric flows in reverse roll coating processes with dynamic wetting lines and air-entrainment: Fene and ptt solutions," *Journal of Non-Newtonian Fluid Mechanics*, vol. 214, pp. 38–56, 2014.

[41] J.-Y. Jang, P.-Y. Chen *et al.*, "Reverse roll coating flow with non-newtonian fluids," *Communications in Computational Physics*, vol. 6, no. 3, p. 536, 2009.

[42] K. Kim, T. Nam, and Y. Na, "A numerical study of the ink transfer process for roll-to-roll printing applications," *Proceedings of the Institution of Mechanical Engineers, Part C: Journal of mechanical engineering science*, vol. 226, no. 10, pp. 2496–2509, 2012.

[43] A. C. Team, *Best Practice for Modeling Thin Liquid Film Coating Flows in ANSYS Fluent*, ANSYS inc., Canonsburg, PA, USA, 2009.

[44] A. fluent Core Team, *ANSYS fluent theory guide*, ANSYS inc., Canonsburg, PA, USA, 2013.

[45] A. C. Team, *ANSYS fluent user's guide*, ANSYS inc., Canonsburg, PA, USA, 2013.

[46] J. Greener, T. Sullivan, B. Turner, and S. Middleman, "Ribbing instability of a two-roll coater: Newtonian fluids," *Chemical Engineering Communications*, vol. 5, no. 1-4, pp. 73–83, 1980.

[47] E. Szczurek, M. Dubar, R. Deltombe, A. Dubois, and L. Dubar, "New approach to the evaluation of the free surface position in roll coating," *journal of materials processing technology*, vol. 209, no. 7, pp. 3187–3197, 2009.

[48] J. H. Lee, S. K. Han, J. S. Lee, H. W. Jung, and J. C. Hyun, "Ribbing instability in rigid and deformable forward roll coating flows," *Korea-Australia Rheology Journal*, vol. 22, no. 1, pp. 75–80, 2010.

[49] Y. Chong, P. Gaskell, and N. Kapur, "Coating with deformable rolls: An experimental investigation of the ribbing instability," *Chemical engineering science*, vol. 62, no. 15, pp. 4138–4145, 2007.

[50] G. Ascanio, P. Carreau, E. Brito-De La Fuente, and P. Tanguy, "Forward deformable roll coating at high speed with newtonian fluids," *Chemical Engineering Research and Design*, vol. 82, no. 3, pp. 390–397, 2004.

[51] G. Ascanio and G. Ruiz, "Measurement of pressure distribution in a deformable nip of counter-rotating rolls," *Measurement Science and Technology*, vol. 17, no. 9, p. 2430, 2006.

[52] G. Ascanio, P. Carreau, and P. Tanguy, "High-speed roll coating with complex rheology fluids," *Experiments in fluids*, vol. 40, no. 1, pp. 1–14, 2006.

[53] M. Sasaki, M. Miyake, and N. Nakata, "Visualization study of flow stability in reverse roll coating," *ISIJ International*, vol. 55, no. 4, pp. 863–869, 2015.

[54] S. K. Han, D. M. Shin, H. Y. Park, H. W. Jung, and J. C. Hyun, "Effect of viscoelasticity on dynamics and stability in roll coatings," *The European Physical Journal Special Topics*, vol. 166, no. 1, pp. 107–110, 2009.

[55] C. Tiu, L. Wang, and T.-J. Liu, "Non-newtonian effects on pre-metered reverse roll coating," *Journal of non-newtonian fluid mechanics*, vol. 87, no. 2-3, pp. 247–261, 1999.

[56] C. Varnam and C. Hooke, "Non-hertzian elastohydrodynamic contacts: An experimental investigation," *Journal of Mechanical Engineering Science*, vol. 19, no. 5, pp. 189–192, 1977.

[57] O. Cohu and A. Magnin, "Experimental investigations on roll coating with deformable rolls," in *The Mechanics of Thin Film Coatings*. World Scientific, 1996, pp. 179–188.

[58] O. Cohu and A. Magnin, "Forward roll coating of newtonian fluids with deformable rolls: an experimental investigation," *Chemical engineering science*, vol. 52, no. 8, pp. 1339–1347, 1997.

[59] P. Gaskell, G. Innes, and M. Savage, "An experimental investigation of meniscus roll coating," *Journal of Fluid Mechanics*, vol. 355, pp. 17–44, 1998.

[60] C.-H. Chien and J.-Y. Jang, "Numerical and experimental studies of thin liquid film flow between two forward-rollers," *Journal of mechanical science and technology*, vol. 21, no. 11, p. 1892, 2007.